Naval Research Laboratory

Washington, DC 20375-5000

NRL Memorandum Report 6586

Texture Segmentation Using Localized Spatial Filtering

LI-JEN DU

Systems Control and Research
Radar Division

January 26, 1990

SECURITY CLASSIFICATION OF THIS PAGE

REPORT DOCUMENTATION PAGE

Form Approved
OMB No 0704-0188

1a REPORT SECURITY CLASSIFICATION UNCLASSIFIED	1b RESTRICTIVE MARKINGS
2a SECURITY CLASSIFICATION AUTHORITY	3 DISTRIBUTION / AVAILABILITY OF REPORT Approved for public release; distribution unlimited.
2b DECLASSIFICATION / DOWNGRADING SCHEDULE	
4 PERFORMING ORGANIZATION REPORT NUMBER(S) NRL Memorandum Report 6586	5 MONITORING ORGANIZATION REPORT NUMBER(S)
6a NAME OF PERFORMING ORGANIZATION Naval Research Laboratory 6b OFFICE SYMBOL (If applicable) Code 5380	7a NAME OF MONITORING ORGANIZATION
6c ADDRESS (City, State, and ZIP Code) Washington DC 20375-5000	7b ADDRESS (City, State, and ZIP Code)
8a NAME OF FUNDING / SPONSORING ORGANIZATION Office of Naval Research 8b OFFICE SYMBOL (If applicable) ONR	9 PROCUREMENT INSTRUMENT IDENTIFICATION NUMBER
8c ADDRESS (City, State, and ZIP Code) Arlington, VA 22217	10 SOURCE OF FUNDING NUMBERS PROGRAM ELEMENT NO: 61153N PROJECT NO: RR021-05-43 TASK NO: WORK UNIT ACCESSION NO:

11 TITLE (Include Security Classification)
Texture Segmentation Using Localized Spatial Filtering

12 PERSONAL AUTHOR(S)
Du, Li-Jen

13a TYPE OF REPORT	13b TIME COVERED	14 DATE OF REPORT (Year, Month, Day)	15 PAGE COUNT
Final	FROM _____ TO _____	1990 January 26	39

16 SUPPLEMENTARY NOTATION

17 COSATI CODES			18 SUBJECT TERMS (Continue on reverse if necessary and identify by block number)
FIELD	GROUP	SUB-GROUP	

19 ABSTRACT (Continue on reverse if necessary and identify by block number)

Spatial filters based on two-dimensional Gabor functions are applied to the image segmentation problem using textural differences for discrimination. In order to provide class separability, the textural content of a scene must have spatial variations which exhibit characteristic differences in frequency and/or directional bandwidths. This idea stems from discoveries in vision research that the Gabor functions model effectively the architecture of the neural receptive fields in the striate visual cortex and in the belief that such functions can play an important role in the analytical study of machine vision, pattern recognition and image processing. This new technique in image segmentation does not required burdensome machine data processing as compared with other techniques based on pixel classification. In this paper the technique is applied to some SAR images of the open ocean surface and of some ice fields. The results are very encouraging.

20 DISTRIBUTION / AVAILABILITY OF ABSTRACT	21 ABSTRACT SECURITY CLASSIFICATION
☒ UNCLASSIFIED/UNLIMITED ☐ SAME AS RPT ☐ DTIC USERS	UNCLASSIFIED
22a NAME OF RESPONSIBLE INDIVIDUAL Li-Jen Du	22b TELEPHONE (Include Area Code) (202) 767-2003 22c OFFICE SYMBOL Code 5380

DD Form 1473, JUN 86 *Previous editions are obsolete* SECURITY CLASSIFICATION OF THIS PAGE

S/N 0102-LF-014-6603

CONTENTS

TEXTURE SEGMENTATION USING LOCALIZED SPATIAL FILTERING

Introduction

Texture is a term used to indicate the spatial intensity variations in scenes or images. The subject has been studied extensively for the purpose of identifying objects or regions of interest. It has been used as a technique to classify images belonging to different categories of objects or regions[1,2]. Despite its clear cut semantic meaning, texture is a rather vaguely defined concept. There is still no unique definition of texture and no systematic approach to its characterization or measurement. There are just too many different kinds of textures in the images of natural or man-made objects to generalize the problem. Most successful texture discrimination techniques developed so far are based on a spatial-statistical approach. In this approach, pixels in a selected neighborhood having special spatial relations are chosen to yield statistical data samples. A variety of numerical measures are then employed to extract the useful information necessary for differentiation. The decision as to which technique is more powerful and accurate depends quite often on the specific images selected for a study.

In a texture segmentation procedure, texture discrimination techniques are used to separate and identify regions of different textures in images. The most commonly used method is to classify each pixel individually. Pixel classification requires a determination of the texture in the pixel's immediate neighborhood. The size of the neighborhood window chosen to process the texture features has to be large enough to provide a statistically meaningful sample. This approach will work provided that an effective discriminant function exists for the textures to be segmented and that the texture extends over a region much

Manuscript approved August 30, 1989.

larger than the window dimension. Also, the neighborhood window has to be scanned over the whole image in order to classify each pixel. It is likely that this process will consume too much time to be realistic in practical applications.

In this paper a new, faster, computational approach to texture analysis and segmentation is presented based on localized spatial filtering. This approach works well in those images where different texture classes differ significantly in their dominant spatial frequencies. Filters are chosen for each class of texture with parameters to match class frequency, bandwidth and the spatial orientation. The filtering process generates filtered images which reveal the relative dominance of each class over the whole image. Segmentation is accomplished by designating each pixel as belonging to the class whose filter produced the strongest response at that location. It is a process whereby image regions of different textures are separated by sensing the localized changes of spatial frequency and its orientations. SAR images of the open ocean surface and of arctic ice regions were chosen to test its applicability. Excellent results are obtained. Comparisons are made with the results obtained from a method based on the co-occurrence matrix approach.

Two-dimensional Gabor Approach to Image and Vision Research

The spatial filters which will be used in this texture analysis and segmentation study are the two-dimensional Gabor functions. The original idea was first introduced by Gabor in 1946[3]. Instead of describing communication signals in terms of idealized time domain and frequency domain functions, he suggested that a more appropriate and realistic approach should be something intermediate between the two extremes. The scheme he proposed to decompose and

represent an arbitrary signal consists of a set of elementary signals which are harmonic oscillations modulated by a probability pulse. To achieve the minimum possible product of the effective duration and the effective frequency width, Gabor chose the gaussian probability function as the modulating envelope. These elementary signals can be written in the following form,

$$f(t)=\exp[-(t-t_0)^2/4\sigma^2]\times\exp[(j2\pi f_0(t-t_0)] \tag{1}$$

where $j=\sqrt{-1}$. These signals are centered at time $t=t_0$ and at frequency $f=f_0$. The gaussian envelope is described by the standard deviation σ. The effective duration of the signal, Δt, is defined as

$$\Delta t=[\overline{(t-t_0)^2}]^{1/2} \tag{2a}$$

and the effective frequency width, Δf, as

$$\Delta f=[\overline{(f-f_0)^2}]^{1/2} \tag{2b}$$

in which the horizontal bar denotes an average value. These Gabor elementary signals possess the property of minimizing the combined effective spread in both time and frequency. Mathematically, this corresponds to an uncertainty relation

$$\Delta t\Delta f\geq 1/4\pi. \tag{3}$$

This information uncertainty relation derived by Gabor indicates that a signal's

characteristics specified simultaneously in time and frequency, is fundamentally limited by a lower bound on the product of its bandwidth and time duration. The family of signals in (1) achieves the theoretical lower limit of this joint uncertainty.

The recent discovery that the measured receptive field profile of single cortical cells matches well the spatial variation of such signals, pointed to the usefulness of Gabor elementary signals in vision studies[4]. Simple cells in the visual cortex have spatially localized receptive fields which consist of distinct elongated excitatory and inhibitory zones[5]. The spatial frequency domain study also revealed the fact that the cells are tuned to specific frequencies with bandwidths of the order of one octave[6,7]. These results match the psychophysical experimental evidence that the visual scene is analyzed in terms of independent frequency channels[8]. The representation of an image in the visual cortex must, therefore, involve both space and spatial frequency variables in its description. Gabor signals provide such dual variable dependence simultaneously. Their special characteristic of maximizing localization in space and in spatial frequency seems to agree with the biological system's natural tendency to sense the environment with optimum efficiency.

Gabor's original theory was developed for studying one-dimensional time-varying communication signals, whereas image and vision related processes occur in two-dimensional(2D) space. The necessary extension of Gabor's scheme to two dimensions was published by Daugman in 1985[9]. In addition to the spatial resolution and spatial frequency bandwidth descriptions, the two dimensional version of the Gabor signals also includes the orientation bandwidth and the width/length aspect ratio characteristics inherent in 2D problems. These 2D Gabor signals also preserve the property of optimum joint information resolution

in the 2D spatial and 2D spectral domains. Supported by the evidence in the biological studies, it is possible that the 2D filters generated by the 2D Gabor elementary signals with the properly chosen parameters could be used for the efficient extraction of various kinds of information from images.

If the spatial and spectral increments are properly chosen, the Gabor elementary functions form a complete mathematical set[10,11]. An image can be decomposed exactly as a summation of clusters of Gabor elementary functions scattered in a uniform lattice structure over the spacial extent of the image. Thus, for instance, image data compression is possible by eliminating those functions with insignificant coefficients and reconstructing the image with the rest. The required calculation is quite intensive and to be of practical use special hardware is needed in which the fundamental algorithms used in the scheme are incorporated in an integrated circuit design.

Texture Discrimination by Gabor Filters

In this paper, the Gabor scheme is used in a task of image segmentation based on texture differences. The contents of the image to be processed are assumed to contain several kinds of image textures portraying physically different objects, landscapes or terrains. Recently, Bovik et al and Turner used the Gabor elementary functions as localized spatial filters in texture discrimination and segmentation of images composed of synthetic textures[12,13,14]. A similar approach is followed in this paper for segmenting SAR images of ocean surfaces and arctic ice regions. The goal of this effort is to search for efficient techniques based on texture analysis to separate and possibly identify areas of different meteorological conditions in the ocean surface case and to reveal ice composition and location in the arctic.

Usually in order for an image segmentation process by texture analysis methods to be feasible there are a few practical conditions to be satisfied. First, the number of different kinds of textures which co-exist in the image must not be large. Second, different kinds of textures are separated by smooth boundaries. Third, there is at least a texture classification approach which can separate the different kinds of textures with reasonable accuracy. For the Gabor filter approach to be applicable, the textures involved should be distinguishable in terms of different localized spatial frequencies and/or in terms of different aspect ratios of these variations in two perpendicular spatial directions.

The geometry of the problem is illustrated in Fig. 1 where two coordinate systems are displayed. The unprimed coordinate system matches that of the image and the axes of the primed coordinate system coincide with the axes of an ellipse shown. The two systems are related by an angle of rotation ϕ. The 2D version of equation (1) can be written in the primed coordinate system as

$$h(x',y')=(1/4\pi\lambda\sigma^2)\exp\{-[(x'/\lambda)^2+y'^2]/4\sigma^2\}\exp[j2\pi(U'x'+V'y')]. \quad (4)$$

It represents a complex sinusoidal grating modulated by a 2D gaussian function profile with aspect ratio λ, scale parameter σ, and the major axis of the ellipse along the x' coordinate direction. Also U' and V' are the spatial sinusoidal frequencies of the grating in the direction of the x' and y' coordinates respectively. The frequency spectrum, which is the Fourier transform of (4), is given by

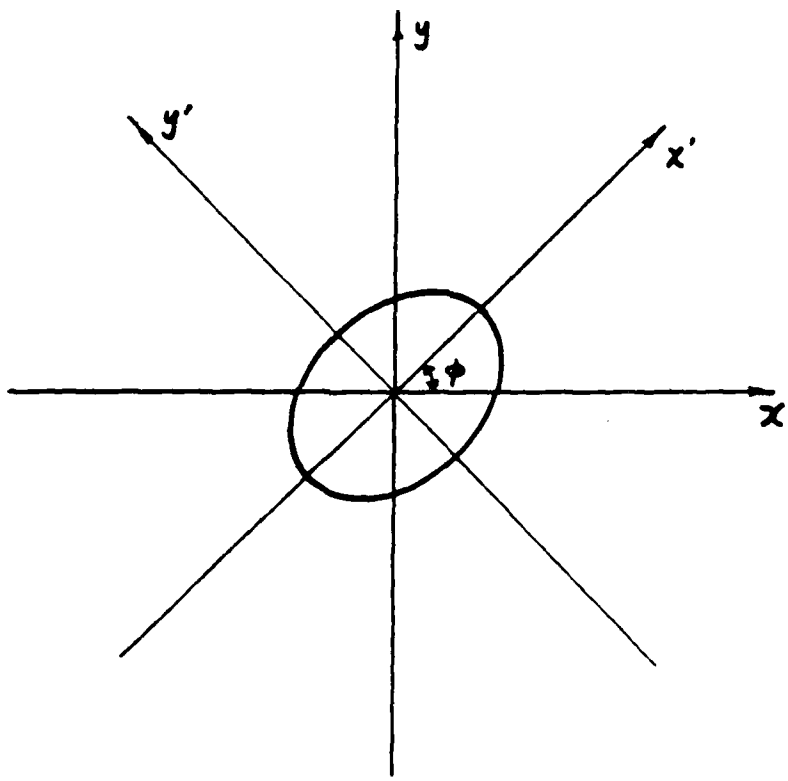

Fig. 1. The coordianate system.

$$H(u',v')=\exp\{-4\pi^2\sigma^2[(u'-U')^2+(v'-V')^2]\}. \qquad (5)$$

The variables in the two coordinate systems are related by the transformation relation,

$$\begin{pmatrix} x \\ y \end{pmatrix} = \begin{pmatrix} \cos\phi & -\sin\phi \\ \sin\phi & \cos\phi \end{pmatrix} \begin{pmatrix} x' \\ y' \end{pmatrix} . \qquad (6)$$

The same relation also holds between the frequency variables (u,v) and (u',v'), and between (U,V) and (U',V'). Note that H(u',v') is a band pass gaussian function with the same aspect ratio λ, except that the orientations of the major and minor axes are interchanged as compared with that in the spacial domain. The radial center frequency $F=(U'^2+V'^2)^{1/2}=(U^2+V^2)^{1/2}$ is measured in cycles per pixel and is oriented at an angle $\theta=\tan^{-1}(V/U)$ with respect to u-axis.

In general, the orientation of the gaussian modulation function and the direction of harmonic spatial variation yield two independent variables in the Gabor scheme. To simplify the problem, only the special case will be pursued in which the direction of spatial change and the major axis of the gaussian ellipse are the same. In this case the angles ϕ and θ are the same and equations (4) and (5) reduce to

$$h(x',y')=(1/4\pi\lambda\sigma^2)\exp\{j2\pi Fx'-[(x'/\lambda)^2+y'^2]/4\sigma^2\} \qquad (7)$$

and

$$H(u',v')=\exp\{-4\pi^2\sigma^2[(u'-F)^2\lambda^2+v'^2]\}. \qquad (8)$$

There are eight degree of freedom in the specification of a 2D Gabor filter[9]. Therefore, it is difficult to gain any intuitive understanding of how the characteristics of the filters change when these parameters are varied. For the images studied in this paper a simplified version of (7) and (8) will be used wherein the parameters to be varied include the size of the gaussian profile(σ), its aspect ratio(λ), the center spatial frequency(F), and its orientation angle(θ) which coincides with one of the axes of the gaussian ellipse. Fig. 2 shows the intensity plots of a 2D Gabor filter specified by the real part of (7), displayed as a 512 by 512 pixel image. The center frequency is F=0.1 cycles/pixel and the bandwidth B=.35 octaves. The aspect ratio is λ=1.5. Starting with the upper left plot and following a clockwise sequence, the orientation angle has the value of $\theta=90^0$, 135^0, 45^0, and 0^0. The center of each plot is located at the column and row pixel coordinates of (128,128), (384,128), (384,384), and (128,384). Fig. 3 is the frequency domain counterpart of Fig. 2. It is also a 512 by 512 pixel image with the same locations for the plot centers and a scale of one pixel distance equal to a spatial frequency of 0.002 cycles/pixel.

For a typical 2D spatial filter, the definition of bandwidth and its associated physical meaning can be quite complicated. In the special case as represented by equations (7) and (8) with spectrum shown in Fig. 3, the problem is simple and clear. There are two bandwidths to be defined. The first is the spatial frequency bandwidth and the second is the orientation bandwidth. The meaning of the parameters introduced to describe and specify them can be made by reference to Fig. 4 which is similar to the lower right part of Fig. 3. Adopting the conventions used in the physiological vision research, the spatial

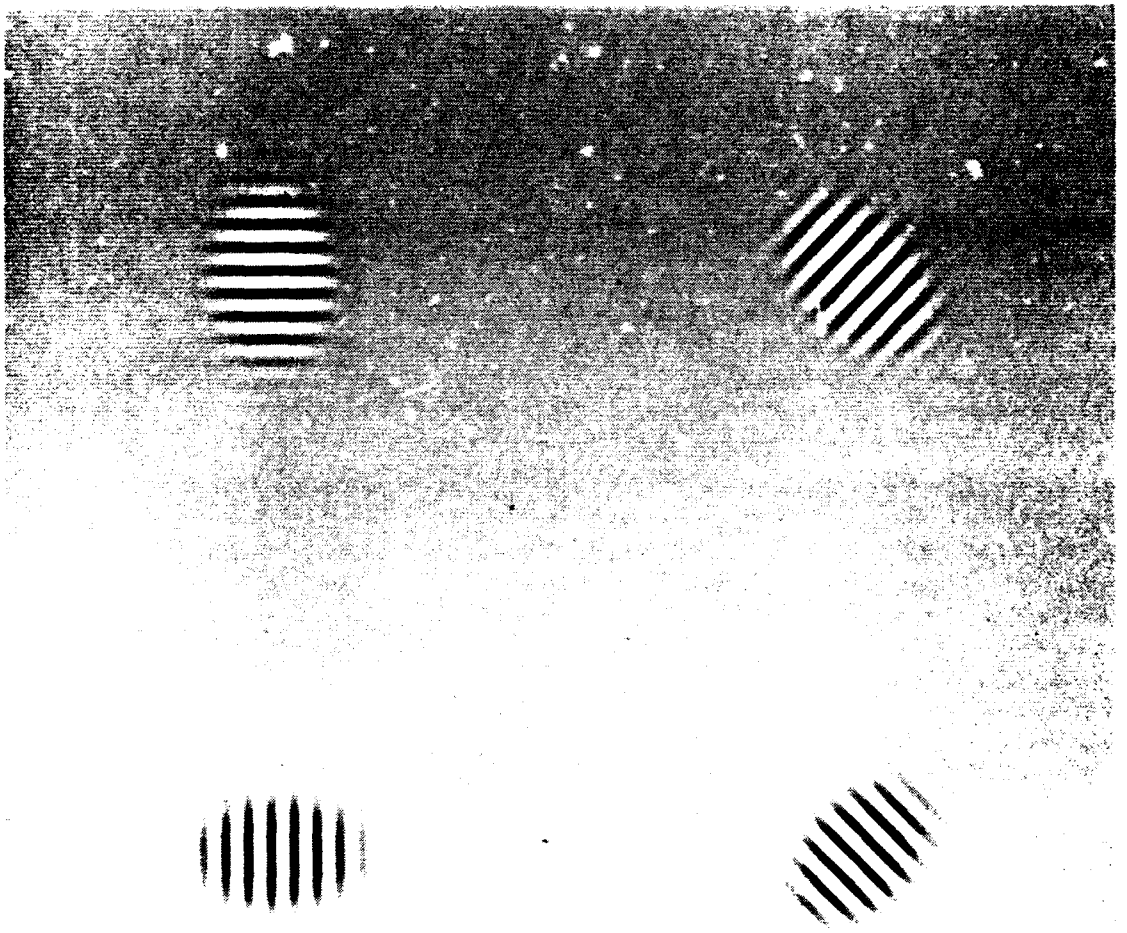

Fig. 2. Intensity plot of the real part of [illegible] filters specified by equation [illegible].

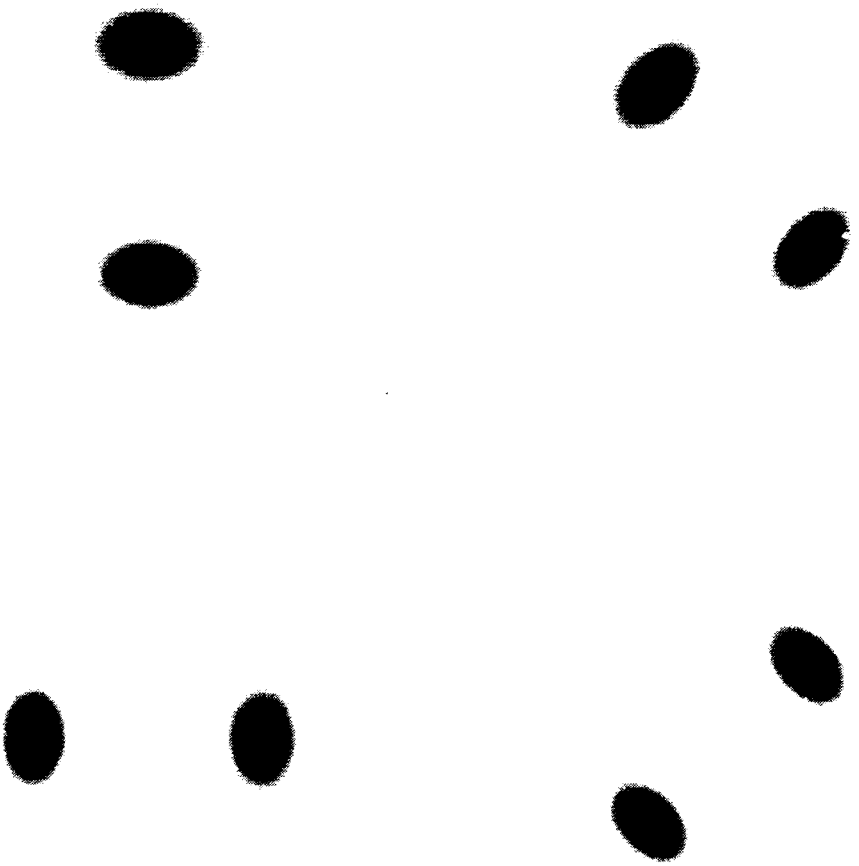

Fig. 3. Frequency spectrum of the 2D Gabor filters specified by equation (8).

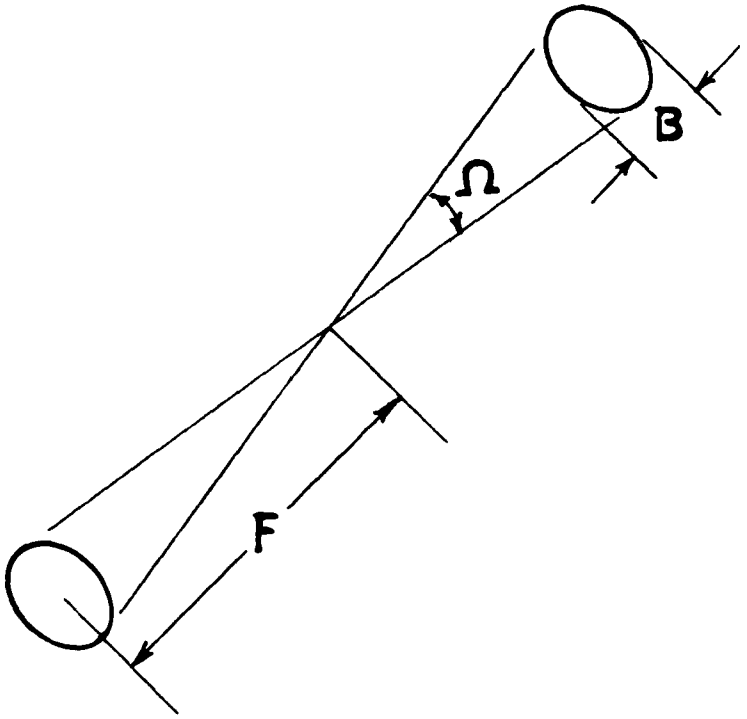

Fig. 4. The bandwidths associated with a 2D spatial filter specified by equations (7) and (8).

frequency bandwidth is measured in octaves which is the ratio of the upper half peak power frequency to the lower half-peak power frequency expressed in terms binary power. The orientation bandwidth is measured in radians. Expressed in terms of the parameters in equation (7) or (8), they are [12]

$$B=\log_2(\pi F\lambda\sigma+\alpha)/(\pi F\lambda\sigma-\alpha)] \tag{9}$$

and

$$\Omega=2\tan^{-1}[\alpha/\pi F\sigma] \tag{10}$$

where $\alpha=[\ln 2/2]^{1/2}$. Also B and Ω can be used to replace σ and λ as two of the four parameters in the filter specification.

The filters expressed by (7) and (8) are rather narrow special cases of the general form of the 2D Gabor filter family. Some conclusions derived from this model, especially those relating to the orientation bandwidth, the spatial frequency bandwidth and the aspect ratio, match quite well the empirical observations recorded in vision research[9,16,17]. These facts confirm the validity of equations (7) and (8) as the proper functions delineating the perception functions of cells in the mammalian visual cortex. It is expected that the model will be useful as an analytical tool in many areas of study in image processing. Choosing the model as a filter and performing a convolution process with an image yields a complex-valued image containing only a limited range of frequencies and orientations specified by its parameters. The filtered image contains mainly components within the bandwidths of the filter. Each pixel's complex magnitude reveals the relative strength of the variations characterized by the filter attributes in its neighborhood in the original image.

Since these filters have the property of achieving the optimum localization in both domains, the filtered image will show the best possible distribution of the spatial signals within the given bandwidths of the filter.

In the problem discussed here, an image is assumed to be composed of several regions or segments. Each region has a dominant textural structure and there are only a few kinds of different textures present. In this situation, the image can be assumed as a summation of weighted Gabor functions of the form expressed in equation (7) with their centers shifted to locations where the corresponding spatial frequencies match the local texture variation. Under this assumption, the image is expanded in a summation of the form,

$$\Phi(x,y)=\Sigma\ a_i h_i(x'-x_i',y'-y_i') +e(x,y) \qquad (11)$$

in which e(x,y) represents the image components whose spatial composition does not match any of the texture categories to be located and identified for segmentation. Also (x_i',y_i') is the center coordinate in the primed system of each localized harmonic spatial textural variation. The integer index i covers all the possible localized texture regions within the image of interest. The functions $h_i(x',y')$ have implicit dependence on variables F_i, σ_i and $\theta_i=\phi_i$. The latter specifies the angle between the primed and unprimed coordinate system. The aspect ratio is assumed to be unity because the spatial variation of the textures to be examined is reasonably isotropic.

Experimental Procedures

In the experiments conducted for this paper, the first step is to identify

the kinds of textures which exist in the image and to locate and separate them from one another or from other regions where there is no texture of interest. The second step is to find ideal or typical training samples. A Fourier analysis is made on the training samples to find the spectral distribution in order to estimate the appropriate parameter values of the Gabor filter functions. The third step is to perform convolutions of the Gabor filter having estimated parameters with the training samples to check the average pixel magnitude of the result in order to determine the best possible combination. If there is more than one texture class in the problem, the convolution is performed between Gabor filters of each class and the training samples of all classes. The parameters of the filters are chosen such that the ratios between the average pixel magnitude of the convolution with the same class and the average pixel amplitudes of convolution with other class samples have the highest absolute values. The convolution is performed using a FFT algorithm. The images which are used for segmentation have a size of 512 by 512 pixels. The FFT is performed on a FPS AP120B 38-bit array processor. The maximum size of a 2-dimensional FFT which can be performed is 128 by 128. Because of the wraparound problem associated with convolution of finite size functions, there are rows and columns around the edge of the filtered window section of the image which have erroneous data[18]. Therefore thirty two pixels of the data around the periphery were discarded after the filtering process of each of the 128 by 128 sub-images. The magnitude of all the Gabor filters used in this study declines to negligible level beyond 32 pixels from their respective centers.

For images in which only one texture class is to be isolated from the background, the segmentation is accomplished by finding an amplitude threshold of the filtered image pixels. For images with several texture classes, the

segmentation is accomplished by assigning each pixel to that class whose Gabor filter produced for it the highest pixel magnitude in the filtered image.

The segmentation process starts at the upper left corner of the image with a 128 by 128 window. Then the window is shifted right by 64 pixels. There is an overlap of 64 columns between the consecutive windows. Since 32 pixels around the periphery have to be discarded in the filtered image, there is no discontinuity in the data required for classification of the inner pixels. After finishing the top row of windows, the same process is repeated in the rows of windows shifted downward by 64 pixels with respect to upper row.

Experimental Results

Fig. 5a shows a SAR image of the ocean surface. It is a sub-image obtained during SIR-B mission of October 11, 1984. The area covered is centered around geographical coordinate of 37^0 North and 74^0 West off the U.S East coast. The whole image looks quite homogeneous. However, by careful examination of the intensity variations, directional striations can be found in it. The areas with the striations may indicate regions on the ocean surface where stronger waves and winds may have existed at the moment the image was generated. The objective of segmentation is to use the computer to map the image automatically into striated and non-striated areas. This image was segmented earlier using the co-occurrence matrix method approach and the texture energy transform method approach[19,20]. Excellent results were obtained with the texture energy transform method, but the results using the co-occurrence matrix method were less satisfactory. Fig. 5b shows the segmented image based on localized spatial filtering with the Gabor filter. The white regions are the striated areas and

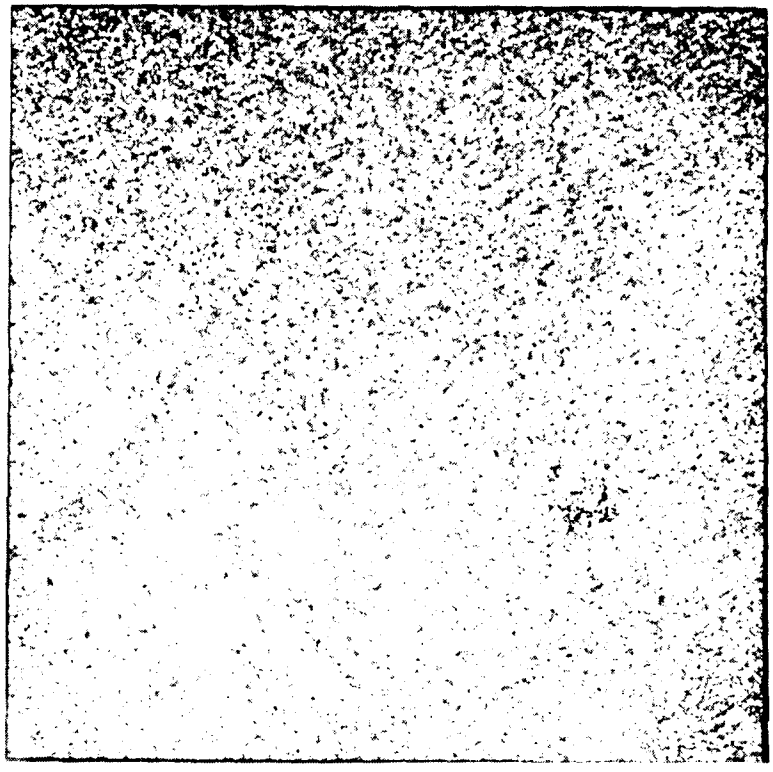

(a)

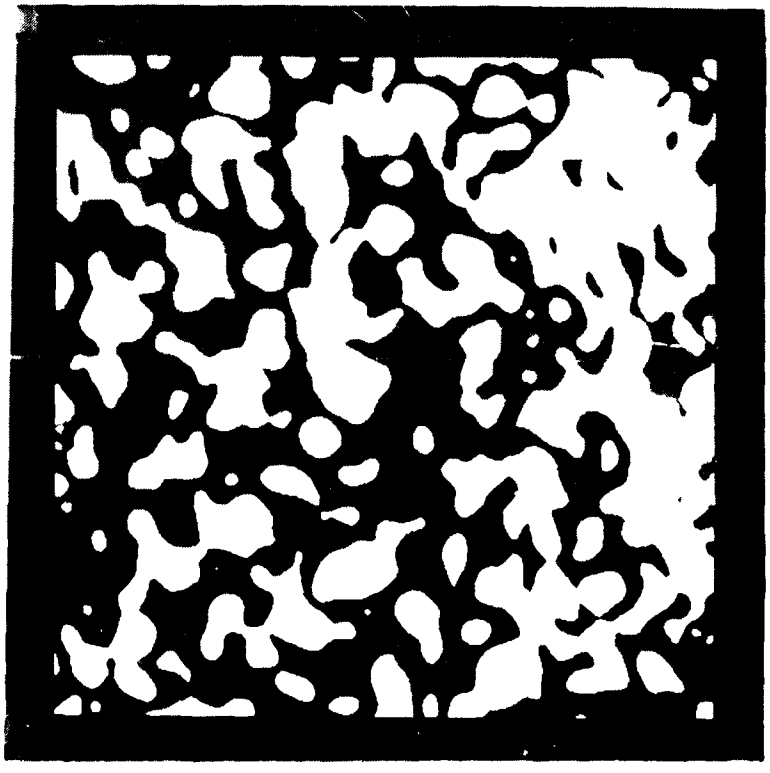

(b)

Fig. 5. (a) SIR-B image of ocean surface. (b) Segmented image of (a).

the dark ones are non-striated. The filter parameters chosen were,

F=0.1328125 cycles/pixel

B=.5 octaves

$\theta=\phi=-65^0$.

These parameters are estimated by examining the FFT result of the training sample in a window of 128 by 128 pixels with the upper left pixel located at column 337 and row 65. The column number is counted from left to right and the row number is counted from top to bottom.

Fig. 6 is a SAR sub-image of an arctic ice region obtained by the SEASAT SAR instrument. Within this image, there are approximately four different kinds of texture corresponding to the images of water, new forming ice, older ice, and multi-year ice. This classification is based on an intuitive understanding of the problem and not upon dependable ground truth data, which are not available. Fig. 7 shows the segmented image. Pseudo colors are used for better visualization. Brown color is assigned to multi-year ice, green color to older ice, cyan color to new forming ice and blue color to water. The training samples used to determine the parameters of the Gabor filters are within windows of size 64 by 64 pixels with the upper left corner located at row 293 and column 374 for multi-year ice, row 27 and column 128 for older ice, and row 231 and column 103 for new forming ice. Water has least prominent spatial variations compared with the ice and no filter was designed for it. Since the FFT operation on each training sample reveals the relative spectral distributions within the sample only and no information for different ices can be extracted from it, a coefficient is attached to each filter as a variable to be adjusted. The factor $1/4\pi\lambda\sigma^2$ in equation (7) is ignored to simplify the problem. These filter

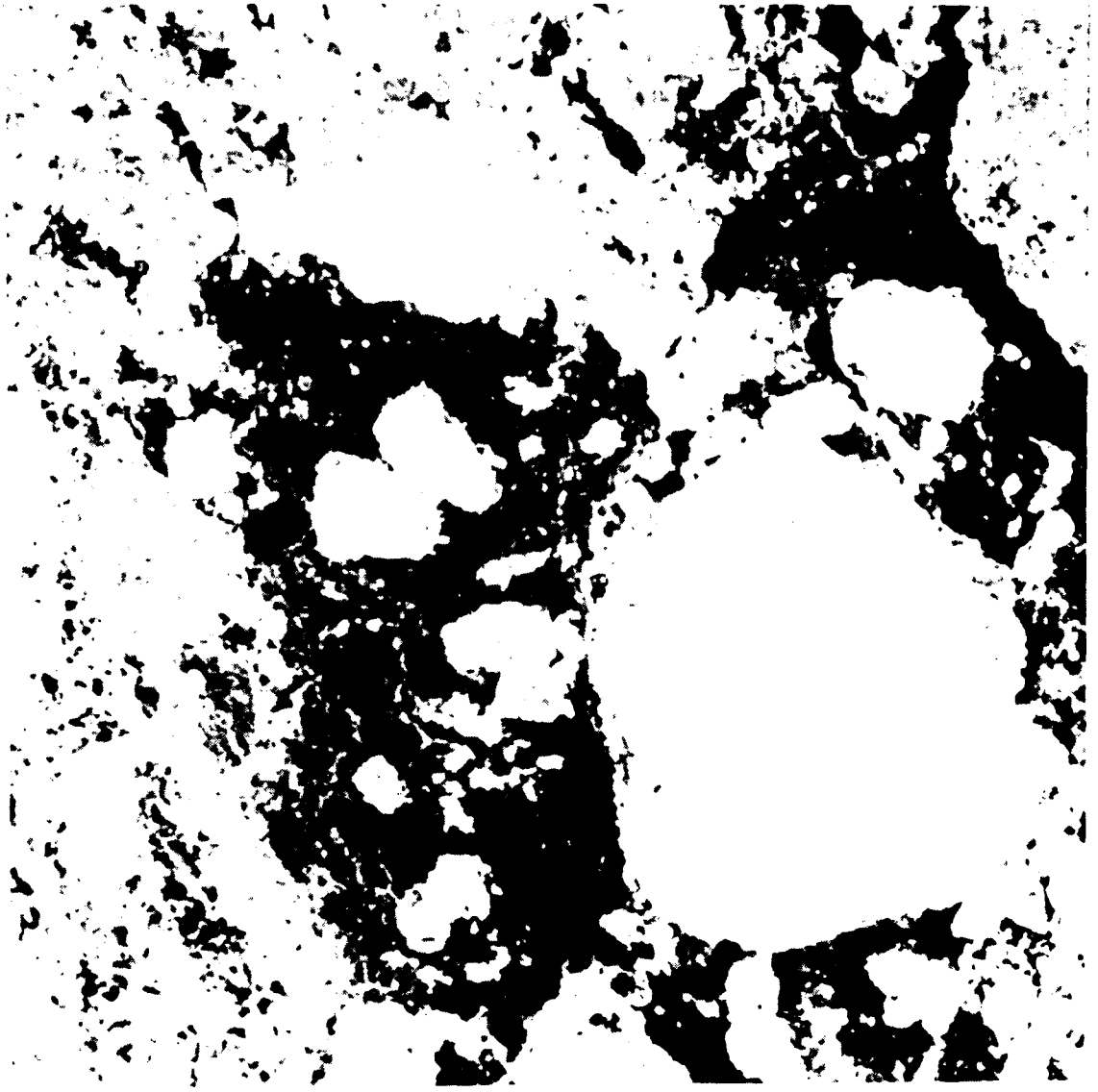

Fig. 6. SEASAT image of arctic ice region.

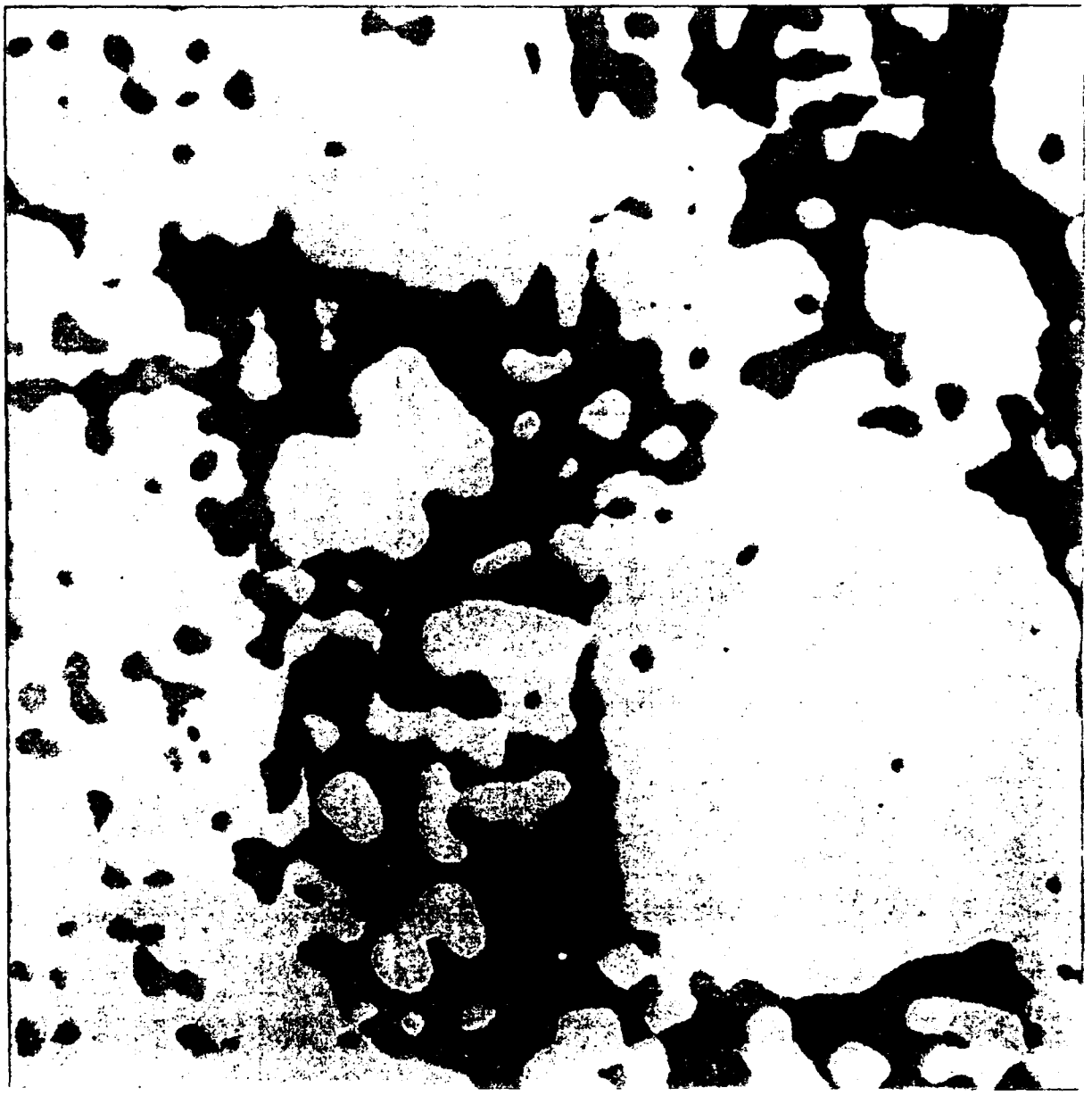

coefficients were determined during segmentation trials to produce the optimum results. The image texture of these ices does not possess any directional characteristics. Four filters are chosen for each kind of ice to cover the harmonic spatial variations in four directions shown in Fig. 2 and 3, other parameters being identical. In the segmentation process, the sum of four filtered image pixel magnitudes from filters of each kind of ice are compared. Each pixel is assigned to the ice category whose filters produced the largest sum. A threshold level of this sum is located in the process to separate ices and water. Although these ices have quite distinguishable appearances on the image, their spectral distributions are sufficiently close to make the decision on the filter parameters non-trivial. Table I lists the filters used to obtain Fig. 7. Fig. 8 shows the segmented images using one of each of the four filters. Fig. 9 shows the segmented image using two filters with harmonic spatial variations in the vertical and horizontal directions. As these textures have no preferred directional characteristics, segmentation using only one filter in a particular direction results in an image which separates the different textural regions quite well except that the filter imposes an emphasis on one direction. With two perpendicular filters, the directional emphasis disappears and the result is a good substitute for the one obtained with the four filters. The coefficients of these filters are the same and the threshold levels separating the ices and the water in Fig. 8 and Fig. 9 are respectively one quarter and one half that used to obtain Fig.7. For comparison, the image of Fig. 6 was also segmented using the co-occurrence matrix approach and the result is shown in Fig. 10. The same pseudo colors are assigned to the three kinds of ices and water. The red color pixels indicate those locations where no decision could be reached in the classification process. The details of the formulation of the problem

Table I

	multi-year ice	older ice	new forming ice
filter coefficient	1.0	0.8	0.58
center frequency	0.0375	0.0469	0.0297
bandwidth	1.9	0.6	0.9

spatial harmonic variation direction angle(same for all three)

$\theta=\phi=0^0, \pm 45^0, 90^0$

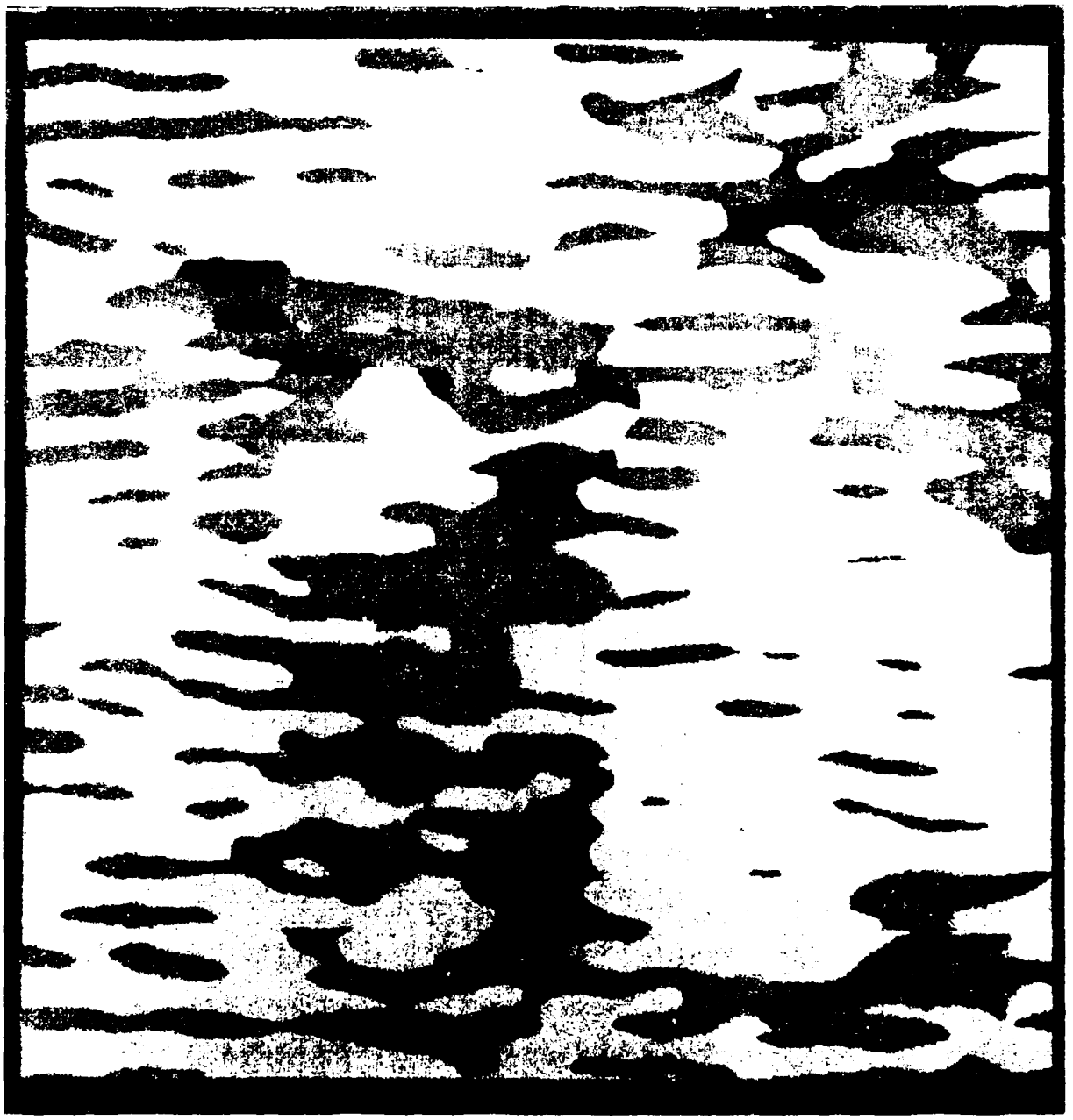

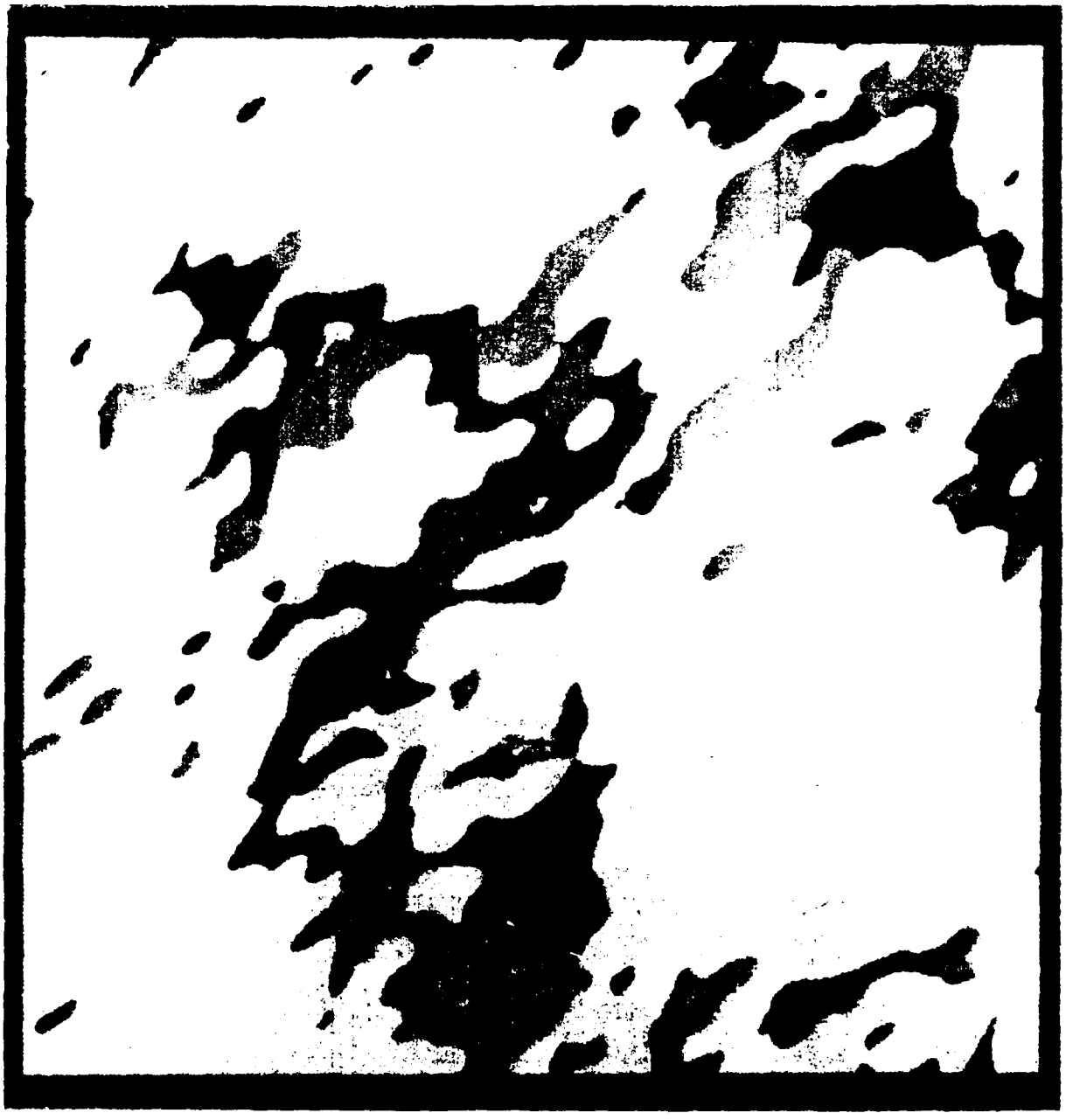

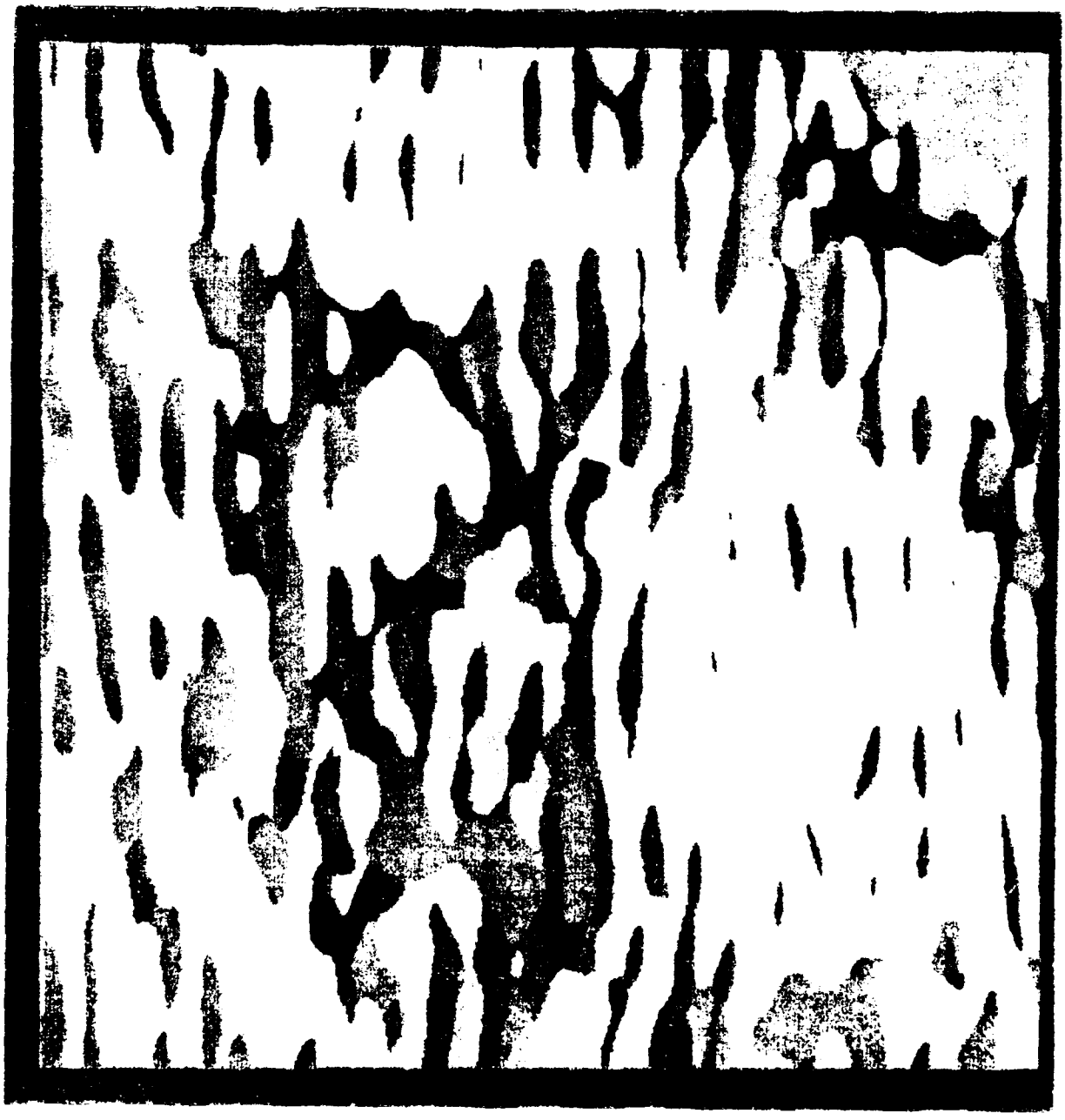

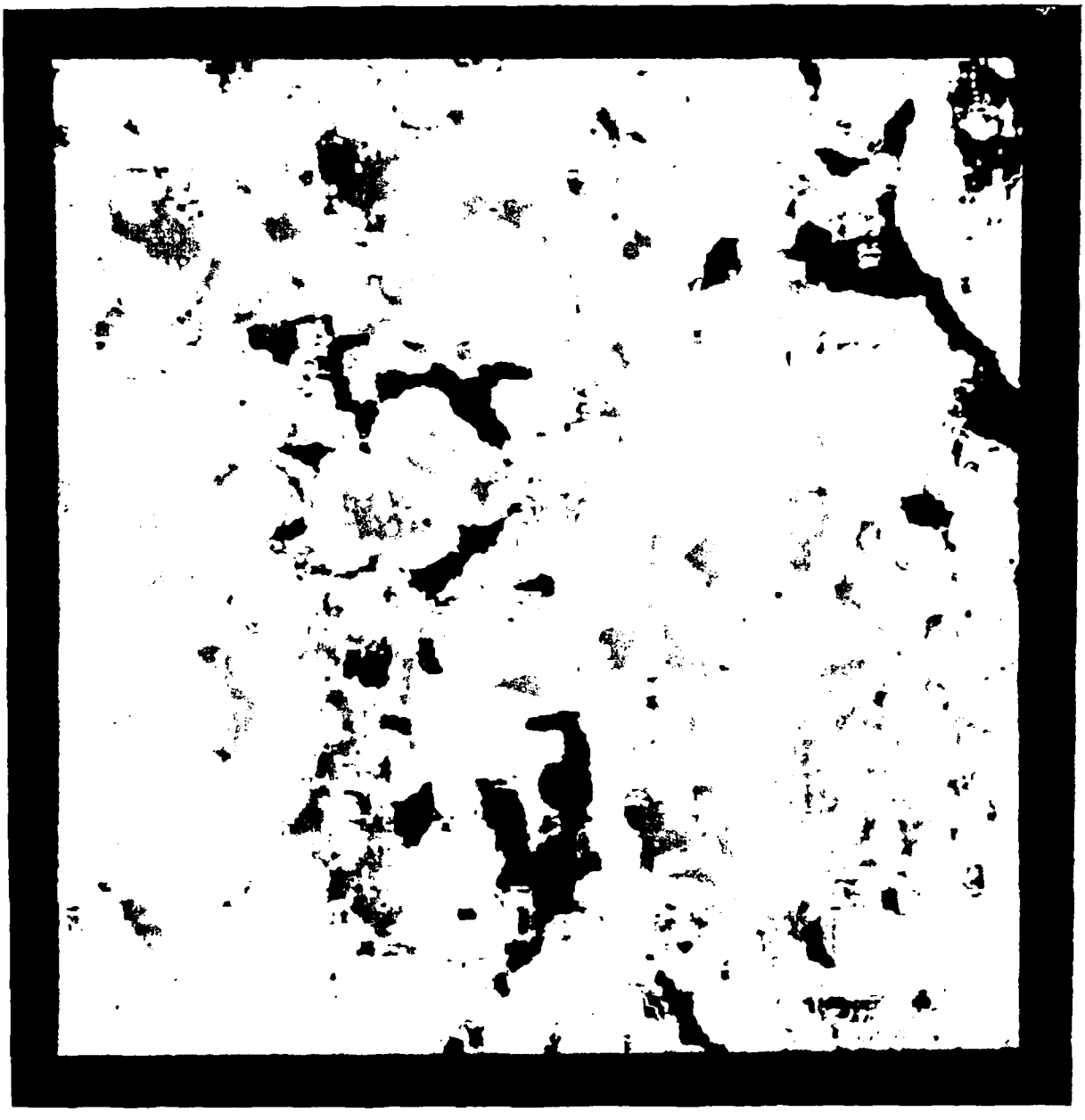

and the steps used in the discrimination process can be found elsewhere[19,20]. The components of the textural features are the averaged values in the four directions(vertical, horizontal, upper right and lower left, upper left and lower right) of the quantities defined in the co-occurrence method as uniformity, correlation, contrast, and inverse difference moment. The discrimination functions used in the classification process are determined from the data samples in the training windows of the image as listed in the Table II. The segmentation is accomplished by a pixel classification process, starting from the upper left corner of the image, and using a window of 13 by 13 pixels. The pixel data within the window were used to evaluate the feature components as the argument for the discrimination function to determine the center pixel's classification. Then the window is shifted toward the right by one position to determine the next pixel's classification. After finishing the whole row of pixels, the same process is continued on the next row with the window shifted downward one pixel. Six pixels along the periphery of the image can not be classified. The size of the window was chosen to be small enough to contain the data necessary to accurately depict the texture characteristics of its center and at the same time large enough to provide reliable statistics. A smaller window size is preferred as it reduces the required computational time. In this case the window size of 13 by 13 pixels was a reasonable compromise.

Comparing these two segmentation results, one concludes that the co-occurrence matrix approach preserves finer texture detail than the approach based on filtering with Gabor functions. But the required computations make it less efficient if faster segmentation is desired. The image shown in Fig. 6 is only a tiny portion of a typical SAR image of an arctic ice area. Although it may have missed revealing the small scale variations of the ice compositions, images

Table II

category	upper left corner pixel		window size	
	column #	row #	column width	row depth
water	176	378	20	23
"	222	376	20	23
"	480	167	32	28
"	439	225	16	16
"	249	359	29	26
new forming ice	134	263	45	45
"	356	104	31	31
"	129	372	32	32
"	123	138	53	38
"	368	58	27	24
older ice	150	218	31	32
"	44	73	24	24
"	480	1	26	26
"	294	383	23	23
multi-year ice	427	343	24	20
"	387	140	31	16
"	82	150	16	16
"	193	82	29	28
"	2	437	33	43
"	9	1	28	39
"	28	346	27	67

segmented by Gabor filters do portray correctly the overall location distribution of different kinds of ice texture in this image. This information provides adequate data to establish ice classification, ice concentration and ice movement which are needed, preferably in real-time, for decisions to be made in year-round arctic operations[22].

The computational time involved in producing the image of Fig. 10, using an optimized code on a typical mini-computer of the VAX 11/780 class, was respectively 1.4, 4.7 and 2.6 times that expended on images in Fig. 7, 8, and 9 with no code optimization.

As mentioned earlier there is no ground truth available for the image in question. Training samples used to determine the discriminant functions in the co-occurrence matrix approach and the filter parameters in the localized filtering approach were picked within the image itself through intuitive judgement. It is easier to select training samples which are homogeneous in textural appearance for the co-occurrence matrix approach since the sample's size and shape can be varied. For the localized filtering approach, using a FFT to find the spectral distribution, the training sample's size has to be a power of two and square in shape. The larger the size the more accurately the parameters can be estimated. A size of 64 by 64 pixels was chosen in this study. It is difficult to find a homogeneous region of the same texture at that size in the image for every kind of ice type. As far as reducing the processing time is concerned, it is not likely that there can be much improvement in the co-occurrence matrix approach. But for the localized filtering approach, significant improvements in computational time seem feasible if the FFT can be performed with larger dimensions and if all the proper filters chosen have smaller spatial extent to reduce the size of the area which has to be overlapped

in the processing.

Concluding Remarks and Discussions

Spatial filtering using 2D Gabor functions is a new approach to the study of texture analysis and segmentation in images. The idea originated in biological vision research and the observation that some of the lower order Gabor functions happen to be the most appropriate mathematical model for describing the 2D receptive field profiles of simple cells in mammalian visual cortex. The Gabor functions posses a unique property of achieving the optimum joint resolution in both the spatial and spectral domains. This fact may be the reason why these functions represent so well the performance of the biological visual systems in optimally sensing and locating objects of different attributes in the visual field. The Gabor functions constitute a complete mathematical set in a combined frequency-position space for image decomposition. Although in general the latter idea may not have practical consequences, some modifications or simplifications of it will have vast potential as a mathematical tool in studies of pattern recognition and machine vision. Textural properties carry useful information in human interpretation of imagery data. Textural analysis involving 2D Gabor functions seems to be a proper approach since it incorporates the physiological knowledge of vision in the formulation of the problem.

In this paper, 2D Gabor functions were used as the spatial filters for the image segmentation based on texture differences. The images under study are assumed to be composed of segments. Each of them has a textural structure belonging to one of a few different kinds. A 2D Gabor function is chosen as the filter to appropriately match the spatial frequency and directional bandwidths of each kind of texture. Convolution of the filter with the image

generates a filtered image of complex magnitude. The variations of the complex magnitude indicates with the best possible spatial accuracy the corresponding textural component's relative strength as a function of location. Segmentation is attained by assigning each pixel to the kind of texture whose filter generates the strongest response at that position. This idea is applied to SAR images of the open ocean surfaces and arctic ice fields. Results obtained are highly promising. Clearly, this technique can be applicable to any image for which segmentation by computer processing, based on textural differences, is desired. Computationally this approach to image segmentation permits fast implementation since the convolution involved can be carried out via Fast Fourier Transform(FFT).

References

[1] Robert M. Haralick, "Statistical and structural approaches to texture", Proc. IEEE, vol.67, pp.786-804, 1979.

[2] Joan S. Weszka, C. R. Dyer, and A. Rosenfeld, "A comparative study of texture measure for terrain classification," IEEE Trans. Syst. Man. Cyber., vol.SMC-6, pp.269-285, 1976.

[3] D. Gabor, "Theory of communication," J.I.E.E., vol. 93, pp.429-459, 1946.

[4] S. Marcelja, "Mathematical description of the responses of simple cortical cells," J. Opt. Soc. Am., vol. 70, pp.1297-1300, 1980.

[5] D. G. Hubel and T. N. Wiesel, "Receptive fields, binocular interaction, and functional architecture in the cat's visual cortex," J. Physiol., London, vol. 160, pp.106-154, 1962.

[6] G. F. Cooper and J. G. Robson, "Successive transformation of spatial information in the visual system," IEE/NPL Conference on Pattern Recognition IEE Conf. Publ., London, vol. 42, pp. 134-143, 1968.

[7] F. W. Campbell, G. F. Cooper, and C. Enroth-Cugell, "The spatial selectivity of visual cells of the cat," J. Physiol., London, vol. 203, pp. 223-235, 1969.

[8] F. W. Campbell and J. G. Robson, "Application of Fourier analysis to the visibility of gratings," J. Physiol., London, vol. 197, pp.551-566, 1968.

[9] J. Daugman, "Uncertainty relation for resolution in space, spatial frequency, and orientation optimized by 2D visual cortical filters," J. Opt. Soc. Amer. (A), vol. 2, pp.1160-1169, 1985.

[10] M. Porat and Y. Y. Zeevi, "The generalized Gabor scheme of image representation in biological and machine vision," IEEE Trans. Pattern Anal. Machine Intell., vol. PAMI-10, pp. 452-468, 1988.

[11] J. R. Higgins, Completeness and Basic Properties of Sets of Special Functions. London: Cambridge University Press, 1977.

[12] A. C. Bovik, M. Clark and W. S. Geisler, "Computational texture analysis using localized spatial filtering," Proc. of Workshop on Computer Vision, pp. 201-206, 1987.

[13] A. C. Bovik, M. Clark and W. S. Geisler, "Multichannel texture analysis using localized spatial filters I: channel demodulation," TR-87-11-43, Computer and Vision Research Center, The University of Texas, December, 1987.

[14] M. Clark and A. C. Bovik, "Texture discrimination using a model of visual cortex," Proc. IEEE Int. Conf. Syst. Man. Cyber., Atlanta, GA, 1986.

[15] M. R. Turner, "Texture discrimination by Gabor functions," Biol. Cybern., vol. 55, pp.71-82, 1986.

[16] R. L. DeValois, D. G. Albrecht, and L. G. Thorell, "Spatial frequency selectivity of cells in macaque visual cortex," Vision Res., vol. 22, pp.545-559, 1982.

[17] J. A. Movshon, "Two-dimensional spatial frequency tuning of cat striate cortical neurons," Abstract of the 9th annual meeting of the Society for Neuroscience, Atlanta, GA, p.799, 1979.

[18] W. H. Press et al., Numerical Recipes, Cambridge: Cambridge University Press, 1986.

[19] L. Du, "Texture study of synthetic aperture radar(SAR) images of ocean surfaces," Naval Research Laboratory, Memorandum Report 6005, September, 1987.

[20] L. Du, "Segmentation of synthetic aperture radar(SAR) images of ocean surface by the texture energy transform method," Naval Research Laboratory,